CELL BIOLOGY

Dermal exosomes containing miR-218-5p promote hair regeneration by regulating β-catenin signaling

Shiqi Hu[1,2], Zhenhua Li[1,2], Halle Lutz[1,2], Ke Huang[1], Teng Su[1,2], Jhon Cores[1], Phuong-Uyen Cao Dinh[1], Ke Cheng[1,2]*

The progression in the hair follicle cycle from the telogen to the anagen phase is the key to regulating hair regrowth. Dermal papilla (DP) cells support hair growth and regulate the hair cycle. However, they gradually lose key inductive properties upon culture. DP cells can partially restore their capacity to promote hair regrowth after being subjected to spheroid culture. In this study, results revealed that DP spheroids are effective at inducing the progression of the hair follicle cycle from telogen to anagen compared with just DP cell or minoxidil treatment. Because of the importance of paracrine signaling in this process, secretome and exosomes were isolated from DP cell culture, and their therapeutic efficacies were investigated. We demonstrated that miR-218-5p was notably up-regulated in DP spheroid–derived exosomes. Western blot and immunofluorescence imaging were used to demonstrate that DP spheroid–derived exosomes up-regulated β-catenin, promoting the development of hair follicles.

INTRODUCTION

People affected by moderate hair loss turn to topical treatments like minoxidil (antihypertensive potassium channel opener) (*1*) and finasteride (dihydrotestosterone-suppressing 5α-reductase inhibitor) (*2*), the only Food and Drug Administration–approved treatments for inducing hair regrowth. Both are designed not for hair loss treatment but serendipity. Researchers kept studying the mechanism of hair follicle cycles and designing small molecular drugs (*3*–*5*), bioproducts (*6*), formulations (*7*, *8*), laser therapy (*9*), and surgical treatment (*10*) since neither minoxidil nor finasteride is very effective. Minoxidil and finasteride require constant reapplication by the user to maintain hair growth (*7*). In their attempts to understand hair regrowth, many researchers have sought a more efficient approach by focusing on the hair follicle cycle. They have tried to stimulate a progression of the follicles from a resting phase (telogen) to an active phase (anagen) (*8*). Instead of follicular unit transplantation, which is costly and sometimes faces a shortage of donor hair follicles, researchers have attempted to use cell therapy to treat hair loss by culturing and proliferating hair follicle cells or mesenchymal cells in vitro and then implanting them in the bald area. In the anagen phase, the hair follicle bulge area is an abundant source of actively growing dermal papilla (DP) cells, which drop out during the resting phase. It has been suggested that hair follicles in bald areas are not disappearing but decreasing in size (*11*). The replenishment of DP cells to bald areas is, therefore, a plausible way to induce the telogen-to-anagen phase transition needed to induce hair growth.

The interactions between the epithelial and mesenchymal cells are vital in regulating the cycle of hair growth (*12*). As the main mesenchymal component of the follicular unit, DP cells induce the transition from telogen to anagen and the formation of new follicles. Thus, regulating DP cells is critical for increasing cell division and follicle growth rate. Two-dimensionally (2D) cultured DP cells have demonstrated no therapeutic effect on hair follicle growth (*13*). It has been reported that 3D spheroid cultures result in a partial restoration of the inductive capabilities of DP cells, which may enable them to induce de novo hair follicles in human skin (*13*). DP cells have to aggregate into hair follicle areas to be effective (*14*). Thus, spheroid culture therapy should be an effective way to regain the capacity for hair regeneration in vitro. However, a comprehensive understanding of the molecular mechanisms that underlie this regenerative process is required. DP cells induce the progression of the hair cycle and regeneration, which requires cross-talk with the surrounding environment (*15*). Exosomes have been extensively investigated because of their role in cell-cell communication and potential in treating diseases (*16*–*18*). The differentially expressed secretome or exosomes from DP spheroids and DP cells could be the key to regulating hair follicle cycles. Recently, DP cell–derived secretome and extracellular vesicles (*8*, *19*, *20*) have demonstrated their effect in promoting hair growth, and their mechanism is under immense investigation. Compared with mesenchymal stem cell–derived exosomes (*8*, *21*), DP cell–derived exosomes were demonstrated to be efficient transforming growth factor–β activators and proven to be important in promoting proliferation of human hair follicle DP cells and hair growth (*22*). 3D culture has been proven to be a way to enrich certain proteins and microRNAs (miRNAs) in secretome (*23*). Young and co-workers (*24*) demonstrated that exosomes derived from 3D DP cells (3D DP-XOs) promoted the proliferation of DP cells and outer root sheath cells and increased the expression of growth factors in DP cells. However, the importance of differentially expressed secretome and miRNAs from 2D DP cells and 3D DP cells and possible mechanisms of 3D DP cells or 3D DP-XOs in promoting hair regeneration have not been demonstrated. In this study, we first verified the hair restoration capacity of DP spheroids in C57BL/6 mice. Then, the therapeutic efficacy of DP secretome was compared with that of the DP spheroids. Different factors and exosomes were expressed when DP cells aggregate. Considering DP cells' aggregative behavior and DP spheroids' ability to induce new hair follicle formation in vivo, we hypothesized that the differentially expressed factors and miRNAs would be previously undefined therapeutics for hair regrowth.

[1]Department of Molecular Biomedical Sciences and Comparative Medicine Institute, North Carolina State University, Raleigh, NC 27607, USA. [2]Joint Department of Biomedical Engineering, University of North Carolina at Chapel Hill, Chapel Hill, NC 27599, and North Carolina State University, Raleigh, NC 27606, USA.
*Corresponding author. Email: kcheng3@ncsu.edu

RESULTS

DP spheroids enhance the expressions of β-catenin and CD133 in vitro and transplantation engraftment in vivo

C57BL/6 mice are widely used in hair physiology studies because, after their backs are depilated, all hair follicles in the area enter the pause phase (catagen) when mice reach 7 weeks old (*25*, *26*). DP cells were isolated from the whiskers of C57BL/6 mice (*27*) and cultured. Passages 3 to 6 were used in this study. Figure 1A shows that DP cells grew out from the hair follicle bulb and exhibited a spindle-like shape when they formed swirly parallel arrays centered on the bulb. After passage, DP cells displayed flattened, polygonal morphology (Fig. 1B). DP spheroids were formed by passaging DP cells into ultralow attachment flasks. The spheroids were 150 to 300 μm in diameter (Fig. 1C and fig. S1) and expressed strong immunofluorescent signals of CD133 (green) and β-catenin (red; Fig. 1D). The expression of CD133 and β-catenin were lower in 2D cultured DP cells (fig. S2). In spheroids, β-catenin expression was enhanced due to the increased cell-cell contact (*13*). CD133-positive DP cells exhibited hair-inducing capacity in vivo (*28*). This was further confirmed via flow cytometry. Enhanced signal intensity can be seen in the gated spheroid cells (fig. S3).

To compare cell survival rates after transplantation, DP cells and DP spheroids stained with DiD (1,1′-dioctadecyl-3,3,3′, 3′-tetramethylindodicarbocyanine, 4-chlorobenzenesulfonate salt) were injected into the depilated backs of C57BL/6 mice. Scaffolds play an important role in 3D cell culture and engineering (*29*). Hair keratins were used as cell culture scaffolds (*8*, *30*), as they are autologous, degradable, and biocompatible. The viability of DP cells was preserved during encapsulation and maintained in the porous microarchitecture of keratin hydrogels. Networks of keratin hydrogels and spheroids self-assembled inside hydrogels are shown in Fig. 1 (E and F), respectively. 2D cells or 3D spheroids were collected and distributed in phosphate-buffered saline (PBS) or keratin hydrogel (10^5 cells/20 μl) for subcutaneous administration. To improve the cell survival rate after transplantation, we compared DP cells/PBS, DP cells/keratin, DP spheroids/PBS, and DP spheroids/keratin

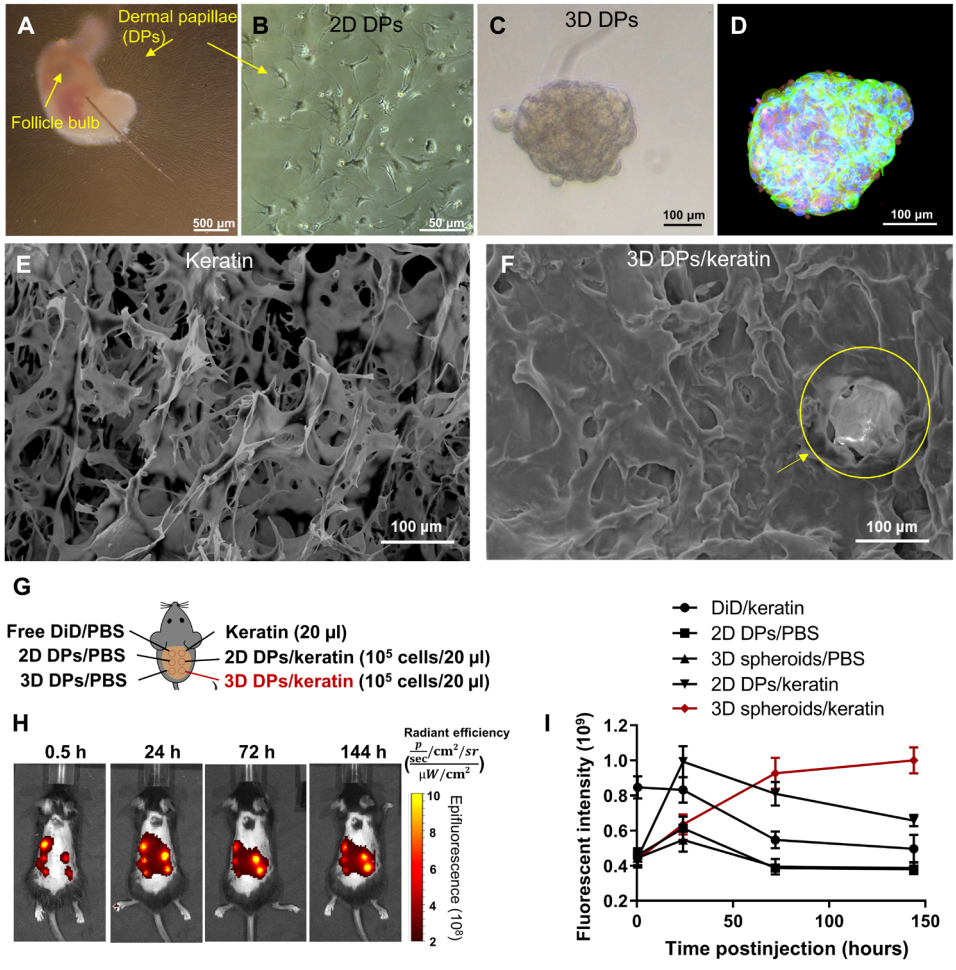

Fig. 1. The preparation and characterization of 3D DP spheroids. (**A**) Isolation of mouse dermal papilla (DP) cells from vibrissae. Scale bar, 500 μm. (**B**) Conventional culture enables the growth of 2D DP cells. Scale bar, 50 μm. (**C**) Growth of DP spheroids in ultralow cell culture flasks. Scale bar, 100 μm. (**D**) Double staining of CD133 (green) and β-catenin (red) in spheroids. Scale bar, 100 μm. (**E** and **F**) Scanning electron microscopy (SEM) images of keratin (E) and 3D spheroid–loaded keratin. (F) One obvious spheroid is highlighted in yellow. Scale bars, 100 μm. (**G**) Schematic illustrating the injection sites on the back of a mouse for the cell retention study. (**H**) The mouse was shaved and injected on the dorsal skin with different formulations as illustrated in (G). Cells were labeled by DiD and then resuspended in PBS or keratin for intradermal injection. In vivo imaging system (IVIS) images were taken at different time points. (**I**) Quantification of IVIS images. Data are shown as means ± SD, $n = 3$ mice. The 3D spheroids/keratin showed the longest retention time.

(Fig. 1G). IVIS (in vivo imaging system) imaging revealed that spheroids demonstrated an enhanced retention and survival rate after injection (Fig. 1, H and I). Spheroids allow higher transplantation rate and functional benefit (*31*, *32*). Keratin further supported cell attachment and proliferation (*8*). DP spheroids/keratin hydrogel maintained high cell viability after engraftment onto the dorsal skin of mice.

DP spheroids enhance the expression of β-catenin, CD133, and Ki67 in hair follicles in vivo

DP cells and DP spheroids were injected into one side of each mouse after depilation (10 one-time injections, evenly distributed on the treated side, 10^5 cells in 20 μl per injection), or 5% minoxidil was topically administered on the treated side daily (Fig. 2A). Ten days later, dorsal skin samples were taken from both the injected sites (left) and nontreated sites (right). β-Catenin, CD133, and Ki67 were stained (Fig. 2, B to D) to compare the hair follicle–inducing mechanism of DP cells, DP spheroids, and 5% minoxidil. Corresponding quantification results are shown in Fig. 2 (E to G).

Minoxidil exerts a vasodilator effect on hair follicles, leading directly to the proliferation of follicle cells (*33*). On the treated side, 5% minoxidil promoted the expression of Ki67 to 37.2% on day 10, but not β-catenin (2.3%) nor CD133 (7.2%), which suggests that the proliferation and growth of whole hair follicle cells were promoted nonspecifically. In contrast, the injection of 2D DP cells enhanced the expression of β-catenin (19.1%) and CD133 (9.8%) on the treated side, and β-catenin (19.9%) and CD133 (6.8%) on the untreated side. Moreover, the injection of 3D DP spheroids enhanced the expression of β-catenin (32.6%) and CD133 (19.1%) on the treated side, and β-catenin (27.8%) and CD133 (13.7%) on the untreated side. Both showed cell migration on the untreated site and enhanced expressions of β-catenin, CD133, and Ki67 on the untreated side compared with minoxidil. In particular, DP spheroids showed much stronger β-catenin and CD133 staining compared with the DP cell

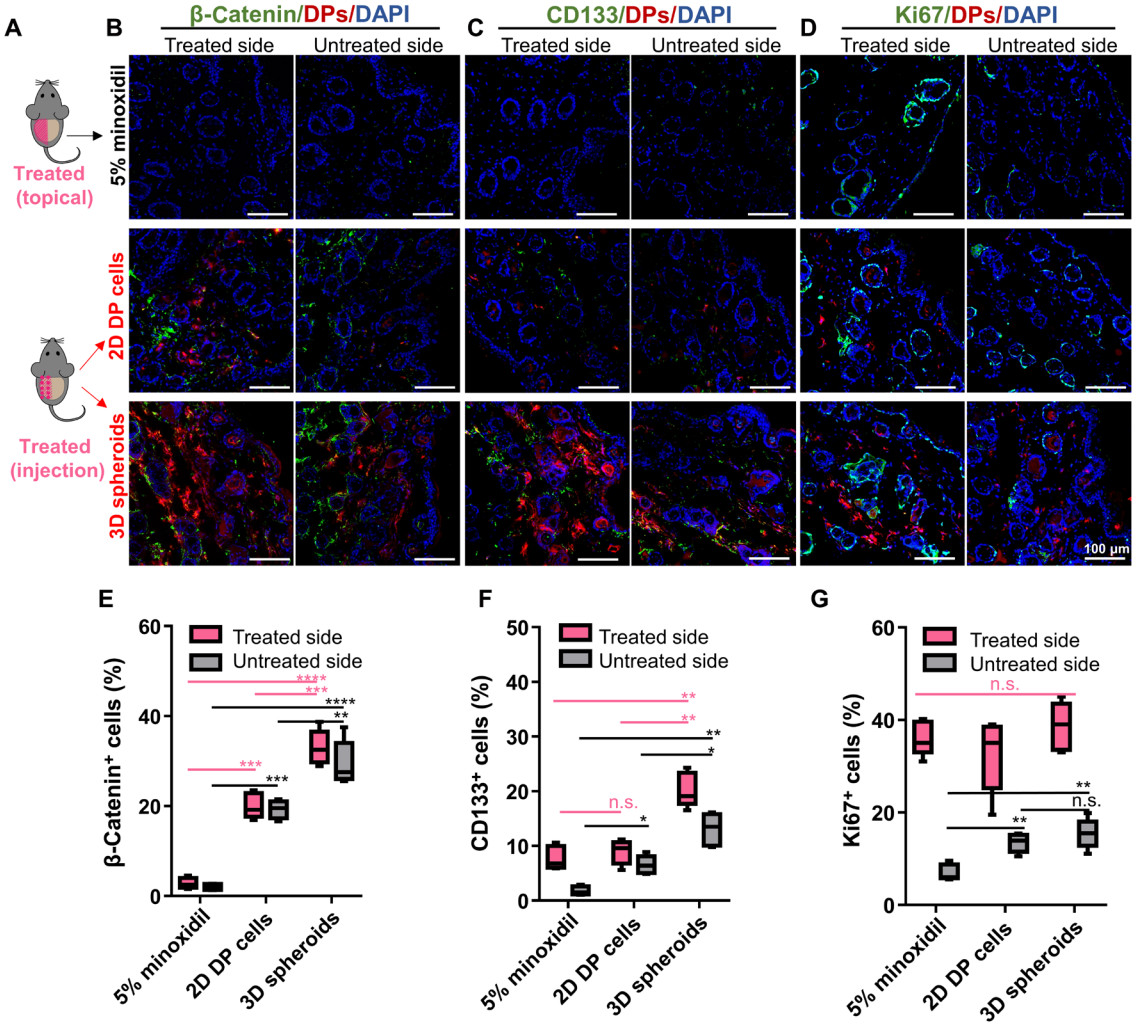

Fig. 2. Comparison of the hair follicle phase with topical treatment of 5% minoxidil against injecting 2D DP cells or 3D spheroids, respectively. (**A**) Illustration of the treatment side (left) and untreated side (right) of a depilated mouse. (**B**) The expression of β-catenin after different treatments at both the treated site and untreated site. (**C**) Representative images showing the expression of CD133 after different treatments at both the treated site and untreated site. (**D**) Representative images showing the expression of Ki67 after different treatments at both the treated site and untreated site. Scale bars, 100 μm. (**E** to **G**) Quantification of β-catenin–positive (β-catenin$^+$) (E), CD133$^+$ (F), and Ki67$^+$ (G) cells. Pink indicates the treated site, and gray indicates the untreated site. $n = 5$; n.s., no significant difference; *$P < 0.05$, **$P < 0.01$, ***$P < 0.001$, and ****$P < 0.0001$.

group. Minoxidil, however, did not alter β-catenin or CD133 expression on either side. The Ki67 signals on the treated side were 37.2, 37.4, and 39.5% for minoxidil, 2D DP cells, and 3D DP cells, respectively, with no significant difference; however, the Ki67 signals on the nontreated side were significantly different at 7.1, 12.6, and 17.5%, respectively. Only the minoxidil group showed a significant difference between the treated side and untreated side. The mechanism of minoxidil is not on regulating DP cells directly but is believed to promote angiogenesis, while the beneficial effects on the untreated sides of DP cell (in PBS or in keratin) groups were likely due to the paracrine effects of injected DP cells. The injection of keratin hydrogel could also promote endogenous DP recruitment by providing a bioactive matrix. Cell migration and viability likely contribute to this remote promotion. This study demonstrated that implanted cells not only influence the hair follicles at the injected site but also regulate the hair follicles in an untreated area. DP spheroid engraftment was more effective in regulating hair follicle growth. In addition, because the migration of cells in the skin was quite limited (fig. S4), paracrine effects could also be an important mechanism in this process.

DP spheroid treatment accelerates hair regrowth in C57BL/6 mice

Minoxidil, the gold standard treatment for hair loss, was used as the positive control. Cultured DP cells were reported to gradually lose their hair-inductive capacity gradually (*4*). We have already showed the limited therapeutic effect of 2D-cultured DP cell administration in Fig. 2. Thus, the hair follicle induction capacity of 3D spheroids was studied here.

We photographed the state of hair regrowth in depilated mice on days 0, 10, 15, and 20 after treatment. The hair growth area was analyzed via morphological observation (Fig. 3, A and B). On day 10, black pigmentation started to show in the minoxidil- and cell-treated groups. All mice in the DP spheroids/keratin group developed much darker skin than the other groups. On day 15, the treated side of the minoxidil group showed 35% fur coverage, compared with just 10% for the untreated side. The DP spheroids/PBS group had an average of 40% fur coverage, and the fur coverage of the DP spheroids/keratin group was approximately 90%. The engraftment and survival rates of cells in PBS were uneven, and so were the resulting therapeutic effects. In contrast, keratin enhanced the overall spheroid engraftment and cell survival rate.

Masson trichrome and hematoxylin and eosin (H&E) staining demonstrated that the DP spheroids/keratin treatment group resulted in larger hair follicles and more collagen distribution compared with the other groups (fig. S5, A and B). The transition of the resting follicles into the anagen phase led to increased follicle size (*34*). In contrast, the control group had smaller follicles and a thinner collagen layer. The injection of DP spheroids did not induce inflammation in the skin tissue because the DP cells were autologous. In addition, the keratin hydrogels did not evoke an acute immune response in vivo.

DP spheroids accelerate the onset of hair follicle anagen phase by up-regulating β-catenin

To elucidate the molecular mechanism, we evaluated the protein levels of β-catenin, extracellular signal–regulated protein kinases 1 and 2 ($Erk^{1/2}$), phospho-$ERK^{1/2}$ ($p\text{-}Erk^{1/2}$), the secreted frizzled-related protein 2 (SFRP2), and glyceraldehyde 3-phosphate dehydrogenase (GAPDH) by Western blot (Fig. 4, A and B) in the depilated dorsal skin 20 days after treatment. The results showed that the expression of β-catenin and $p\text{-}Erk^{1/2}$ in the DP spheroid groups was up-regulated, and that of SFRP2 was down-regulated in comparison to the control and minoxidil groups. The WNT/β-catenin pathway has a critical role in regulating the hair cycle by promoting hair growth (*35*). β-Catenin is a key regulator of hair follicle growth, and it is reported to be the primary initiator of the anagen phase (*36*). SFRP2 has been reported to be involved in several cellular activities and biological processes via the down-regulation of β-catenin in nuclear translocation. These results indicate that DP spheroids may activate hair follicle development by up-regulating β-catenin signaling in the WNT pathway. We also performed immunofluorescence staining of SFRP2 and β-catenin (Fig. 4, C to E) to further confirm the down-regulation of SFRP2 and up-regulation of β-catenin in the spheroids/keratin group. Thus, 3D spheroid culture could be an effective strategy to improve DP therapeutic potency before it is administered as a hair loss treatment.

Comparison of protein and miRNA profiles between DP cells and DP spheroids

DP spheroids affected not only the local injection site but also the regulation of the hair follicle cycle in a nontreated area due to paracrine signaling. DP cells stimulate follicular development and modulate mesenchymal-epithelial interactions by releasing various growth factors and exosomes (*24*, *37*) (Fig. 5A). Exosomes and secretome from DP cells and DP spheroids were isolated and detected. Compared with the other treatment groups, spheroid secretome resulted in significantly higher expression levels of basic fibroblast growth factor (bFGF) and tissue inhibitor of matrix metalloproteinase 2 (TIMP2; fig. S6). Transmission electron microscopy (FEI Talos F200X) images showed the morphology of exosomes (Fig. 5B). The average size of DP cell–derived exosomes (DP-XOs) was around 180 nm, and the average size of DP spheroid–derived exosomes (DP spheroid–XOs) was around 130 nm (Fig. 4C). Figure S7 indicates the identifying exosomal makers: Alix, CD9, and CD81. To compare miRNA content in the exosomes, we performed miRNA arrays and found that DP spheroid–XOs expressed miR-218-5p at significantly higher levels than DP-XOs (Fig. 5D and fig. S8).

As shown in Fig. 5E, bFGF can be accepted by cell membrane–bound FGFR and up-regulate the expression of $p\text{-}Erk^{1/2}$, which up-regulates the expression of β-catenin (*38*). TIMP2 was known to inhibit the expression of matrix metalloproteinase 2 (MMP2) (*39*), which might hinder the migration and proliferation of DP cells (*40*). However, the mechanism behind MMP2-mediated regulation of hair follicles is still not clear and needs to be further studied. Growth factors are involved in the promotion of hair growth cycles, and the bFGF mechanism has been demonstrated before (*41*, *42*). bFGF and TIMP2 levels were approximately doubled in spheroid secretome compared with 2D cell secretome. In addition, miR-218-5p in 3D DP-XOs was up-regulated 25-fold in comparison with 2D DP-XOs. Thus, determining how exosomes regulate this process and the importance of miR-218-5p in mediating the hair cycle was the main focus of this study.

DP spheroid–derived exosome treatment for hair regrowth

Cell-based therapy is a promising step forward in the pursuit of achieving hair follicle neogenesis. However, harnessing of cellular components to be therapeutic catalysts would make for an even more convenient therapeutic product, obviating the cell as the therapeutic

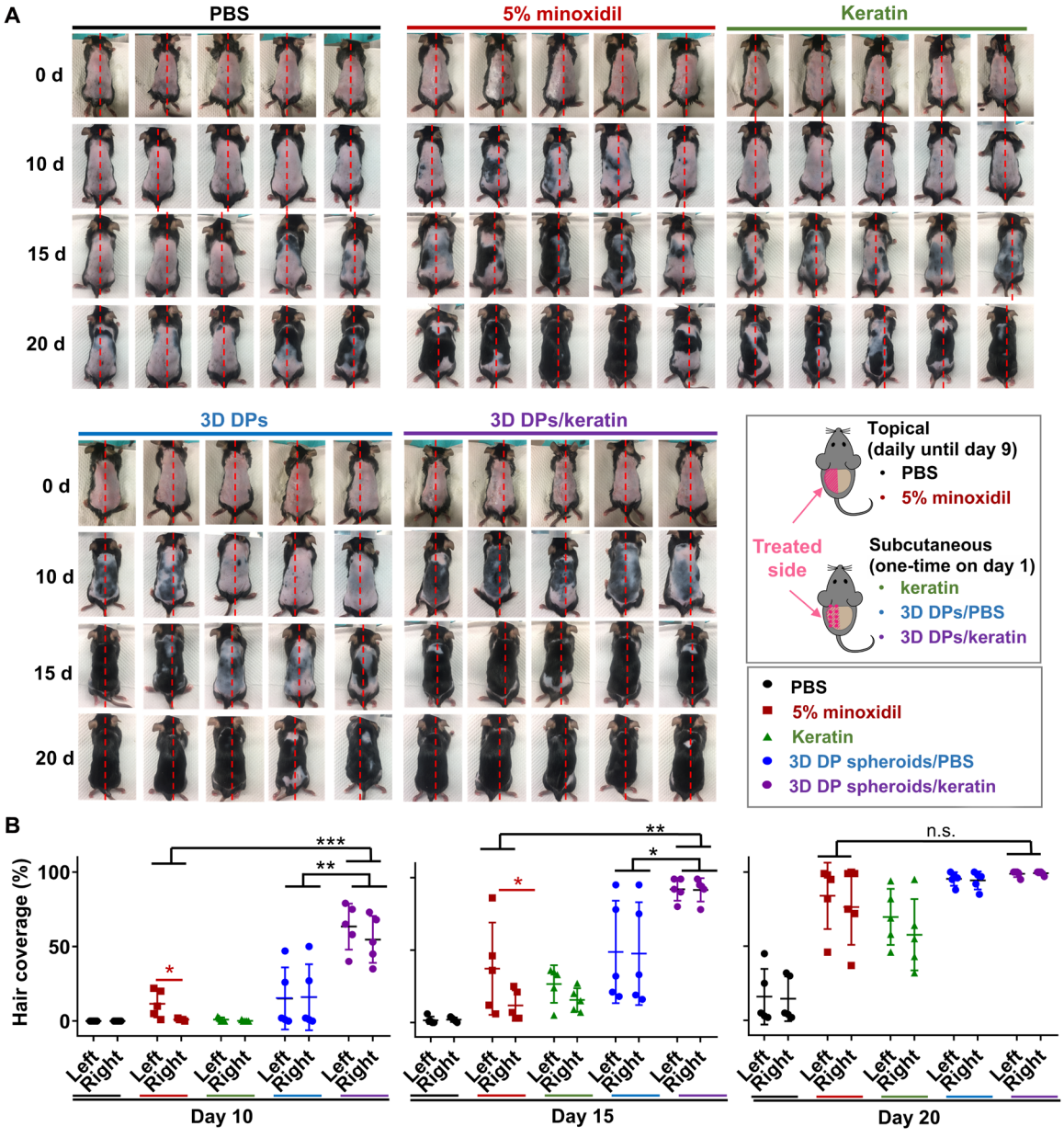

Fig. 3. Dorsal hair growth experiment on C57BL/6 mice. (**A**) Observation of hair coverage. Mice were divided into five groups ($n = 5$) and treated on their left halves. Mice were imaged on days 0, 10, 15, and 20, respectively. (**B**) Quantification of hair coverage on days 10, 15, and 20. Both the left (treated) and right (untreated) sites were recorded. $n = 5$; n.s., no significant difference; $^{*}P < 0.05$, $^{**}P < 0.01$, and $^{***}P < 0.001$. Photo credit: S.H., North Carolina State University.

carrier. Both exosomes and secretome might contribute to the hair growth process, while differentially expressed miR-218-5p in exosomes might contribute to the higher efficacy of 3D spheroids in promoting hair growth compared with 2D DP cells. Also, according to literature, miR-218-5p directly targets SFRP2, and thus, it up-regulates the WNT/β-catenin pathway (*43*). Therefore, miR-218-5p up-regulated exosomes were the main research object in this study.

The recruitment of DP cells to the hair follicle is crucial to hair regrowth (*44*). We demonstrated that spheroid-derived exosomes could effectively promote DP migration compared with exosomes from 2D cells (fig. S9), and enhanced cell mobility could also be important to their aggregate and migration behavior in vivo (*45*). Then, in vivo studies were performed on C57BL/6 mice. Exosomes were administrated to one side of the dorsal skin (Fig. 2A) and compared with a 5% minoxidil topical treatment. In morphological observation (Fig. 6A) and corresponding quantification (Fig. 6B), the therapeutic efficacy of 2D DP-XOs was not significantly different from that of minoxidil, while 3D DP spheroid–XOs accelerated hair growth to an extent that was comparable to cell treatment. To explore the changes of SFRP2 and β-catenin expression in the skin after treatment, we harvested dorsal skin samples from different groups on day 15. Immunostaining confirmed that β-catenin expression was increased in the groups treated with DP spheroid–XOs when compared with those treated with 2D DP-XOs or minoxidil. DP

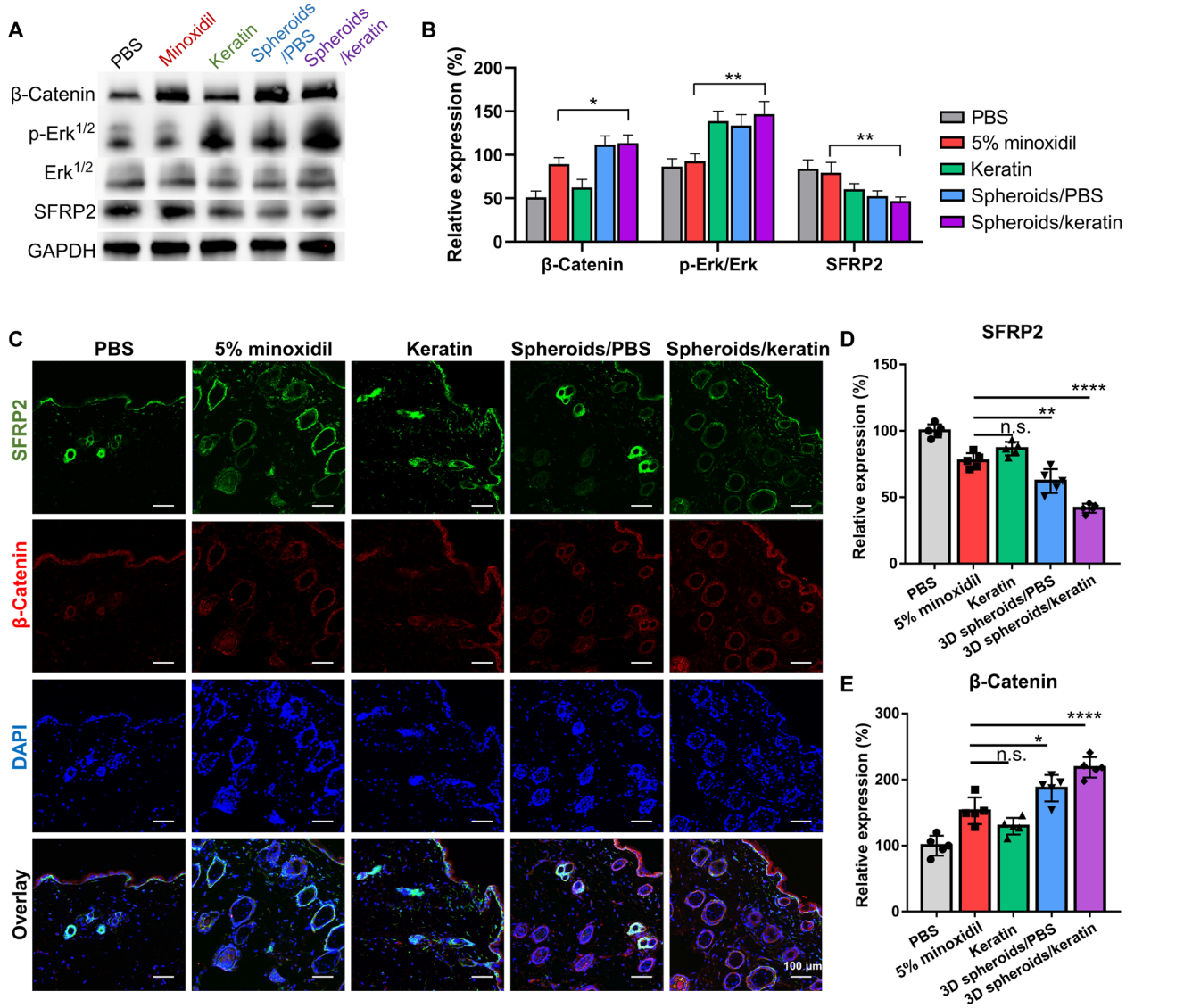

Fig. 4. Western blotting and immunohistology with various treatments. (**A**) Western blot analyzing β-catenin, p-Erk$^{1/2}$, Erk$^{1/2}$, SFRP2, and GAPDH protein content in the dorsal skin on day 20. (**B**) Quantification of Western blot protein levels by group. $n = 3$. (**C**) Immunofluorescence costaining of SFRP2 and β-catenin on skin samples from different treatment groups. Scale bars, 100 μm. (**D**) Quantification of the relative expression of SFRP2. (**E**) Quantification of relative expression of β-catenin. $n = 5$. n.s., no significant difference; $^*P < 0.05$, $^{**}P < 0.01$, and $^{****}P < 0.0001$.

spheroid–XOs can regulate hair growth cycles by down-regulating SFRP2 and up-regulating β-catenin (Fig. 6, C and D). Because miR-218-5p directly targets SFRP2, miR-218-5p mimics and inhibitors were used to further validate the importance of miR-218-5p enrichment.

miR-218-5p plays a crucial role in exosome-mediated hair regrowth

One of the main challenges in miRNA treatment is delivery. The in vitro model does not accurately reflect whether miR-218-5p plays an important role in regulating hair follicle growth when considering the diverse types of cells in the follicles (*46*). Here, an mmu-miR-218-5p mimic was mixed with polyethylenimine (PEI) solution (in vivo-jetPEI; Polyplus Transfection, Illkirch, France) according to the manufacturer's instructions. The PEI/negative control, PEI/mimics, or PEI/inhibitors polyplex solution (10 μl per site) was carefully administered, subcutaneously, into the dorsal skin of depilated mice (Fig. 6E). By targeting SFRP2, miR-218-5p mimics promoted hair follicle development, while miR-218-5p inhibitors inhibited the onset of the anagen phase in the hair follicle cycle. We can see notable hair regrowth effects with the treatment of miR-218-5p mimic, as compared with the control group and the miR-218-5p inhibitors. However, these effects (50 to 90% hair coverage) were less potent than those from exosome treatment (95 to 100% hair coverage) on day 20. We reason that this is because exosomes contain a variety of miRNAs and proteins, and miR-218-5p is not the only one (although a very important one) that was able to contribute to promoting hair growth.

We used a different strategy to promote hair growth. As illustrated in Fig. 6G, both miR-218-5p–loaded exosomes and miR-218-5p mimics encapsulated by in vivo PEI promoted the transcript of miR-218-5p. The genetic structure of miR-218-5p showed that it would target

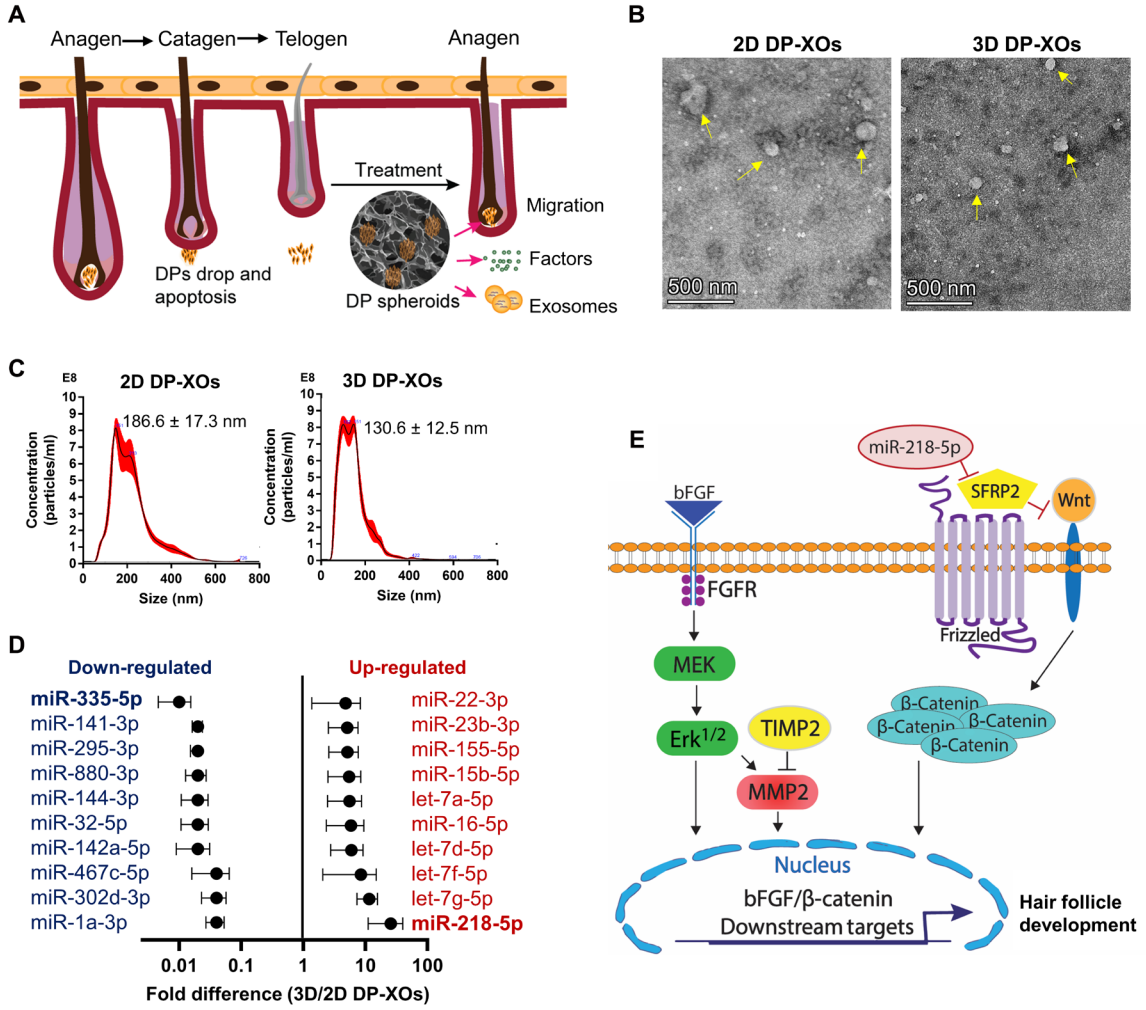

Fig. 5. Secretome from 2D DP cells and 3D DP spheroids. (**A**) Schematic illustrating how DP spheroids promote the hair cycle transition from catagen to telogen via the migration and secretion of factors and exosomes. In anagen, an abundant source of growing DP cells is inside the follicle bulge. DP cells drop during catagen. The replenishment of DP cells promotes the onset of anagen. (**B** to **E**) Characterization of 2D DP-XOs and 3D DP-XOs. (B) TEM images. Exosomes are indicated by yellow arrows. Scale bars, 500 μm. (C) Size distribution by NanoSight. (D) Top 10 up-regulated and 10 down-regulated miRNAs of 3D DP-XOs compared with 2D DP-XOs. ($n = 3$ biological replicate and $n = 3$ technical replicates for each biological replicate). (E) Schematic illustrating FGF2- and TIMP2-driven hair follicle regulation and miR-218-5p–induced promotion of hair follicle development.

SFRP2 directly. To demonstrate the regulatory effect that miR-218-5p and WNT signaling have on the hair growth cycle, we examined transcriptional mediators, SFRP2, and β-catenin by Western blot. Skin samples (day 15) showed that miR-218-5p mimics robustly increased endogenous β-catenin expression, while treatment with miR-218-5p inhibitors showed decreased β-catenin expression (Fig. S10).

Together, these data support the theory that the main therapeutic pathway involves the stimulation of WNT signaling by miR-218-5p–overexpressed exosomes through a down-regulation of SFRP2, a WNT signaling inhibitor, and up-regulation of β-catenin.

DISCUSSION

Given the temporary efficacy of finasteride and minoxidil, and the limited number of treatments available, the need to discover new therapies for preventing hair loss and enhancing hair regrowth is urgent (*47*). Alternative solutions are challenging, especially bioproducts.

Replenishing DP cells with in vitro–cultured DP cells is a reasonable approach for driving the telogen-to-anagen transition in the hair follicle cycle. However, DP cells will lose their hair-inducing capacity over time when they are cultured on a flat, plastic surface. Horne and co-workers (*48*) observed that cultured DP cells (over six passages) could not induce any hair follicles to transition to anagen after implantation in situ. DP cells have to agglomerate in the hair follicle bulb to promote folliculogenesis (*49*, *50*). Osada *et al.* have shown that DP cells regained their hair follicle inductive capacity after they were cultured in suspension as spheroids (*14*). In our study, we verified a higher expression of CD133 and β-catenin in DP spheroids compared with DP cells, which means that DP spheroids could exhibit better hair growth inductive capacity in vivo.

Secretome from DP spheroids is also different from that of dissociated cells. Researchers have shown that dermal spheres are morphologically akin to DP cells in the anagen phase with expression profiles different from 2D cells but greatly similar to intact DP cells

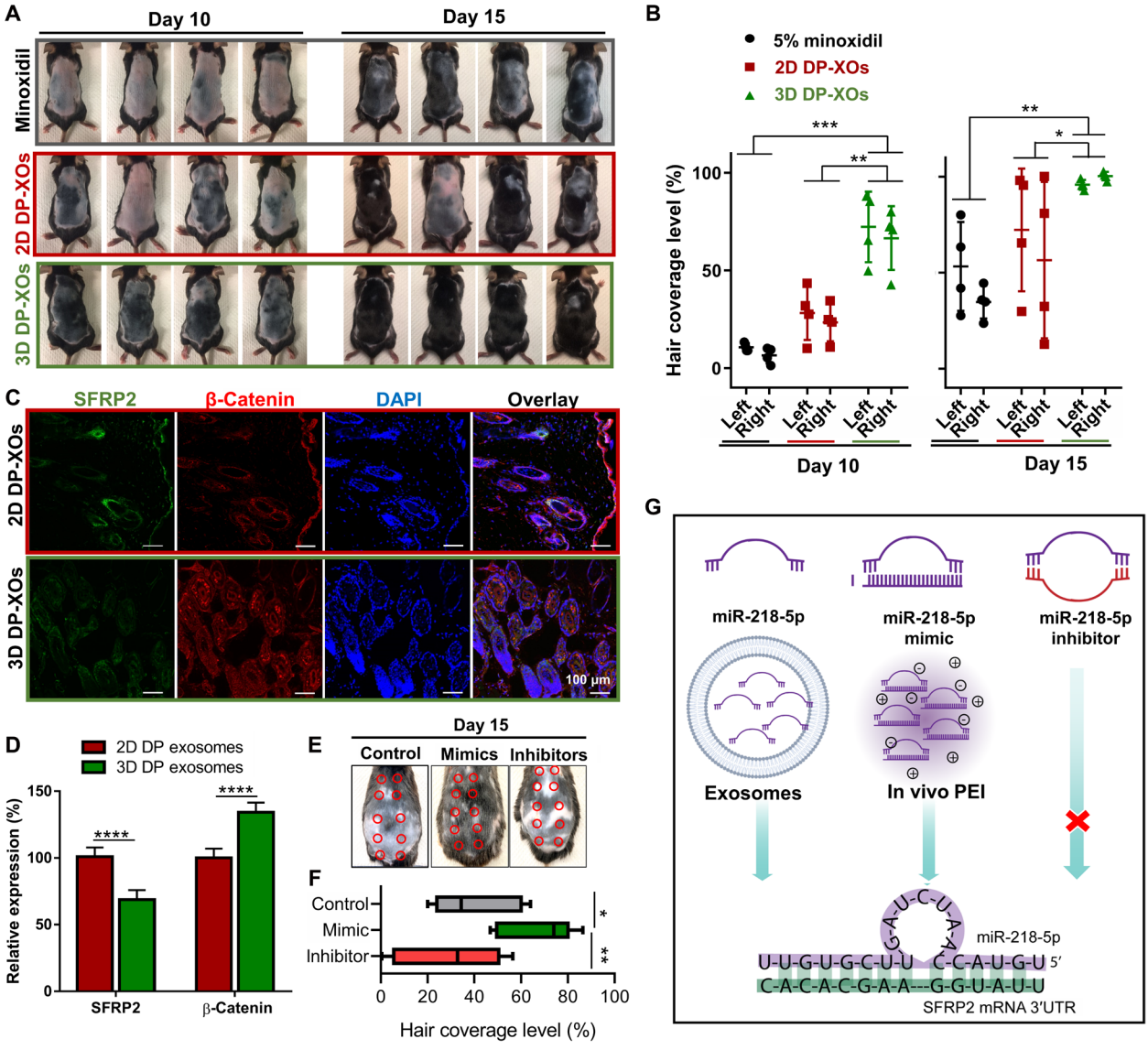

Fig. 6. Effects of exosome treatment on dorsal hair regrowth. (**A**) Mice were divided into three groups ($n = 4$) and treated on their left sides. Mice were imaged on days 10 and 15, respectively. (**B**) Corresponding hair coverage analysis of different groups. Both the left and right sides were recorded. 3D DP-XOs promoted hair follicle growth more effectively than minoxidil and 2D DP-XOs. $n = 4$; $^{*}P < 0.05$, $^{**}P < 0.01$, and $^{***}P < 0.001$. (**C**) Immunofluorescence costaining of SFRP2 (green) and β-catenin (red) on skin samples from different treatment groups. Nuclei were stained by DAPI (4′,6-diamidino-2-phenylindole) (blue). Scale bars, 100 μm. (**D**) Quantification of the relative expression of SFRP2. $n = 5$; $^{****}P < 0.0001$. (**E**) Representative mice imaged on day 20 after injection of negative control, miR-218-5p mimics, and inhibitors, respectively. Red circles indicate injection spots. There is a small bald spot on the injection site, which means that the delivery approach needs further modification. (**F**) Quantification of hair coverage level (%) of three groups on day 15. $n = 4$; $^{*}P < 0.05$ and $^{**}P < 0.01$. (**G**) miR-218-5p up-regulated exosomes and miR-218-5p mimics delivered via in vivo-jetPEI can transfect miR-218-5p to target SFRP2 and thus up-regulate the WNT/β-catenin pathway; miR-218-5p inhibitor will block this signaling to a certain degree. Photo credit: S.H., North Carolina State University.

(*51*). Evidence of how the transplanted hair follicles affect the environment of the bald area and paracrine effects involved were not sufficient. Our studies demonstrated that DP cells exerted their regulatory capacity on hair cycles mainly through a paracrine mechanism. The expression of β-catenin was up-regulated not only in the injection sites but also in nontreated sites. DP cells release various growth factors and vesicles to regulate follicular biology, and it was established that cultivation in spheroids most efficiently preserves the initial phenotype of these cells in vitro. Rather than introducing more DP cells to accumulate into hair follicles, exosomes were injected to regulate hair follicle cycles. Spheroid-derived exosomes, with a higher level of miR-218-5p compared with 2D DP-XOs, also enhanced the expression of β-catenin and down-regulated SFRP2, which positively regulated hair follicle growth and maintained the anagen phase of the hair cycle.

C57BL/6 mice are useful models for screening agents that promote hair growth because their skin produces pigment only during the anagen phase (*52*). Human hair loss has hormonal, environmental, and genetic causes. Because of its complexity, cell or secretome therapy may be more advantageous in treating hair loss compared

with minoxidil, since the primary therapeutic mechanism of minoxidil is the increase in cutaneous blood flow to the treated site. Increased blood flow causes hyperpolarization of cell membranes, allowing more nutrients to reach the follicles and cells. However, if DP cells remain dormant, little hair regrowth is likely to occur. In this study, we demonstrated that spheroids drive the hair cycle from telogen to anagen in healthy mice. Disease-related models or hormone-related hair loss models are needed to fully demonstrate the advantages of exosome therapy in comparison to minoxidil. Another limitation of this study lies in the interaction of exosomes with follicle cells. We focused on animal studies rather than cell studies because we were not sure which types of follicle cells were being regulated. More cell studies are needed to explore mechanisms in the future.

Collectively, we demonstrated that miR-218-5p–overexpressed exosomes accelerated the onset of anagen, and spheroid culture provided a potential avenue for cell therapy. miR-218-5p regulated hair follicle development by down-regulating WNT signaling inhibitor SFRP2, thus promoting β-catenin, creating a positive feedback loop. Our study may offer the following advantages compared with current hair regeneration practice. For people not suitable for invasive surgical procedures, they can benefit from the administration of the factors and exosomes by a minimally invasive approach, e.g., needle-free injection (*23*), microneedle patches (*53*–*55*), and sprays (*56*, *57*). Compared with the commercially available minoxidil, exosomes represent a natural product with fewer side effects. Overall, studies outlined here may represent new therapeutic strategies for hair treatment.

MATERIALS AND METHODS

Isolation of DP cells from C57BL/6 mice

The vibrissa pads were cut off from a euthanized C57BL/6 mouse (*27*) and then rinsed in PBS three times. Hair follicles were dissected and incubated with 0.25% dispase (STEMCELL Technologies) for 20 min in the incubator. Then, a horizontal cut was made above the DP. The hair follicle bulbs were then transferred into a rat-tail collagen I (Sigma-Aldrich)–coated dish. We used Eagle's minimal essential medium (MEM; Gibco), 10% fetal bovine serum (FBS; Corning), 1% penicillin-streptomycin, and bFGF (10 ng/ml; Fisher Scientific) as DP medium until DP cells grew out from bulbs about 3 days later. Then, hair follicle bulbs were washed and placed in fresh medium. DP cells reached confluence after 1 week.

2D cell and 3D spheroid culture

For 2D cultures, rat-tail collagen I–coated flasks were used for passage. Passages 3 to 6 DP cells were used for this study. For 3D culture, DP cells were seeded in an ultralow attachment 96-well plate (Corning, 5×10^4 per well) to count the number spheroids. Spheroids were formed 2 days after seeding. Days 5 to 7 spheroids were used in the animal study.

DP medium [MEM, 10% FBS, 1% penicillin-streptomycin, and bFGF (10 ng/ml)] was used for cell culture. To collect secretome or exosomes, the DP medium was changed to basic MEM medium (no FBS) once cells reached 80% confluence. Then, conditioned medium was collected after 3 days (*23*).

Secretome and exosome isolation and analysis

Secretome was concentrated via Amicon Ultra-15 centrifugal filter units (3-kDa cutoff) and washed with PBS once. Exosomes were concentrated via Ultra-15 centrifugal filter units (100-kDa cutoff) and washed with PBS once.

The mouse Angiogenesis Array (RayBio) and the miRNA PCR (polymerase chain reaction) Array Mouse miFinder (Qiagen) were used according to the manufacturer's instructions.

Preparation of keratin hydrogels

Keratin hydrogel was prepared according to a previous publication, with modifications (*6*). Briefly, human hair (local barber) was washed with water and then cut into small pieces. Then, hair fragments were treated with 2.5% (w/v) peracetic acid overnight before being washed thoroughly with running water. Hair fragments were immersed in 150 mM tris base for 2 hours to extract proteins. Then, a clear solution was obtained after fibers were removed via a 40-μm sieve. This solution was purified by dialysis against DI water (with 3-kDa molecular cutoff dialysis membrane; Fisher Scientific) and freeze dried (lyophilized). The resulting lyophilized solid was further ground into a fine powder. Fifteen percent keratin hydrogels (w/v) were prepared by reconstituting the fine powder with PBS. Spheroids were dispersed in keratin solution and left in a 37°C incubator overnight while the keratin formed a hydrogel.

Scanning electron microscopy

The morphology of the hydrogel was visualized via scanning electron microscopy (SEM). Samples were fixed with 2% glutaraldehyde and then dehydrated in gradient ethanol, successively, for 10 min each. They were then dried in hexamethyldisilazane (Sigma-Aldrich). Gels were sputter coated with gold before imaging (JEOL 6010LA SEM, JEOL Ltd., Japan).

Animals and in vivo studies

Seven-week-old male C57BL/6 mice were purchased from the Jackson laboratory and allowed to adapt to their new environment for 1 week. Hair was removed by using depilatory cream to observe the pink skin (*10*). Then, animals were randomly divided into groups ($n = 5$) to study hair regrowth. Minoxidil was topically applied daily as a positive control. All other treatments were administered subcutaneously. All work with mice was in accordance with the Institutional Animal Care and Use Committee at North Carolina State University.

Cell treatment dose: 1.0×10^6 cells in 200 μl PBS were subcutaneously injected into 10 spots (20 μl per site) on the left side of the dorsal skin.

Exosome treatment dose: 2.0×10^9 exosomes in 200 μl of PBS were subcutaneously injected into 10 spots (20 μl per site) on the left side of the dorsal skin.

Negative control, miR-218-5p mimics, and inhibitors (Sigma-Aldrich) were administered according to the protocol provided by in vivo-jetPEI (Polyplus-transfection). Briefly, mice received 10 injections per depilated dorsal skin. miRNA mimic (400 ng) or inhibitor was dissolved in 90 μl of 5% glucose (w/v) solution, and then 10 μl of in vivo-jetPEI solution was added. The solution was immediately vortex mixed and incubated for 15 min at room temperature before injection. Control groups were injected with mimic control.

Skin tissue histology

Mice were euthanized, and the whole dorsal skin was removed. Skin tissue was fixed in 4% paraformaldehyde and then cut into 5-μm-thick sections by Cryostat. H&E and Masson trichrome were stained according to protocols. For immunofluorescence histochemistry,

the primary antibodies used were mouse anti–β-catenin (Abcam, ab6301), rabbit anti-CD133 (ab19898), rabbit anti-Ki67 (ab16667), and rabbit anti-SFRP2 (ab137560). The secondary antibodies used were goat anti-mouse immunoglobulin G (IgG; Alexa Fluor 488; ab150113), goat anti-rabbit IgG (Alexa Fluor 488; ab150077), and goat anti-mouse IgG (Alexa Fluor 555; ab150114).

Western blot

Samples were loaded and compared with a standard ladder (Precision Plus Protein Standards, Bio-Rad). Primary antibodies were as follows: mouse anti–β-catenin (Abcam, ab6301), rabbit SFRP2 (ab137560), anti-Erk1 (pT202/pY204) + Erk2 (pT185/pY187) [MAPK-YT] (ab50011), anti-ERK1 + ERK2 (ab17942), and anti-GAPDH [horseradish peroxidase (HRP)] (ab9482). Goat anti mouse IgG (HRP) (ab205719) and goat anti-rabbit IgG (HRP) (ab205718) were used.

Statistical analysis

All quantitative experiments were conducted in triplicate unless otherwise indicated. Data were shown as means ± SEM and analyzed by two-tailed, unpaired Student's *t* test for comparison between the two groups. Data comparisons between more than two groups were done by using one-way analysis of variance (ANOVA) followed by the post hoc Bonferroni test. Data between grouped data were analyzed by using two-way ANOVA. Differences with a *P* value less than 0.05 were considered statistically significant.

SUPPLEMENTARY MATERIALS

Supplementary material for this article is available at http://advances.sciencemag.org/cgi/content/full/6/30/eaba1685/DC1

View/request a protocol for this paper from *Bio-protocol*.

REFERENCES AND NOTES

1. A. Rossi, C. Cantisani, L. Melis, A. Iorio, E. Scali, S. Calvieri, Minoxidil use in dermatology, side effects and recent patents. *Recent Pat. Inflamm. Allergy Drug Discov.* **6**, 130–136 (2012).
2. H. Rambwawasvika, P. Dzomba, L. Gwatidzo, Hair growth promoting effect of *Dicerocaryum senecioides* phytochemicals. *J. Med. Chem.* **2019**, 7105834 (2019).
3. S. Inui, S. Itami, Reversal of androgenetic alopecia by topical ketoconzole: Relevance of anti-androgenic activity. *J. Dermatol. Sci.* **45**, 66–68 (2007).
4. R. Sinclair, M. Wewerinke, D. Jolley, Treatment of female pattern hair loss with oral antiandrogens. *Br. J. Dermatol.* **152**, 466–473 (2005).
5. V. Kanti, A. Messenger, G. Dobos, P. Reygagne, A. Finner, A. Blumeyer, M. Trakatelli, A. Tosti, V. Del Marmol, B. M. Piraccini, A. Nast, U. Blume-Peytavi, Evidence-based (S3) guideline for the treatment of androgenetic alopecia in women and in men–short version. *J. Eur. Acad. Dermatol. Venereol.* **32**, 11–22 (2018).
6. V. Cervelli, S. Garcovich, A. Bielli, G. Cervelli, B. C. Curcio, M. G. Scioli, A. Orlandi, P. Gentile, The effect of autologous activated platelet rich plasma (AA-PRP) injection on pattern hair loss: Clinical and histomorphometric evaluation. *Biomed. Res. Int.* **2014**, 760709 (2014).
7. M. J. Gomes, S. Martins, D. Ferreira, M. A. Segundo, S. Reis, Lipid nanoparticles for topical and transdermal application for alopecia treatment: Development, physicochemical characterization, and in vitro release and penetration studies. *Int. J. Nanomedicine* **9**, 1231–1242 (2014).
8. G. Yang, Q. Chen, D. Wen, Z. Chen, J. Wang, G. Chen, Z. Wang, X. Zhang, Y. Zhang, Q. Hu, L. Zhang, Z. Gu, A therapeutic microneedle patch made from hair-derived keratin for promoting hair regrowth. *ACS Nano* **13**, 4354–4360 (2019).
9. Y. Huang, F. Zhuo, L. Li, Enhancing hair growth in male androgenetic alopecia by a combination of fractional CO_2 laser therapy and hair growth factors. *Lasers Med. Sci.* **32**, 1711–1718 (2017).
10. P. T. Rose, The latest innovations in hair transplantation. *Facial Plast. Surg.* **27**, 366–377 (2011).
11. L. A. Garza, C.-C. Yang, T. Zhao, H. B. Blatt, M. Lee, H. He, D. C. Stanton, L. Carrasco, J. H. Spiegel, J. W. Tobias, G. Cotsarelis, Bald scalp in men with androgenetic alopecia retains hair follicle stem cells but lacks CD200-rich and CD34-positive hair follicle progenitor cells. *J. Clin. Invest.* **121**, 613–622 (2011).
12. V. A. Botchkarev, J. Kishimoto, Molecular control of epithelial-mesenchymal interactions during hair follicle cycling. *J. Investig. Dermatol. Symp. Proc.* **8**, 46–55 (2003).
13. C. A. Higgins, J. C. Chen, J. E. Cerise, C. A. B. Jahoda, A. M. Christiano, Microenvironmental reprogramming by three-dimensional culture enables dermal papilla cells to induce de novo human hair-follicle growth. *Proc. Natl. Acad. Sci. U.S.A.* **110**, 19679–19688 (2013).
14. A. Osada, T. Iwabuchi, J. Kishimoto, T. S. Hamazaki, H. Okochi, Long-term culture of mouse vibrissal dermal papilla cells and *de novo* hair follicle induction. *Tissue Eng.* **13**, 975–982 (2007).
15. D. Enshell-Seijffers, C. Lindon, M. Kashiwagi, B. A. Morgan, β-Catenin activity in the dermal papilla regulates morphogenesis and regeneration of hair. *Dev. Cell* **18**, 633–642 (2010).
16. A. C. Vandergriff, J. B. M. de Andrade, J. Tang, M. T. Hensley, J. A. Piedrahita, T. G. Caranasos, K. Cheng, Intravenous cardiac stem cell-derived exosomes ameliorate cardiac dysfunction in doxorubicin induced dilated cardiomyopathy. *Stem Cells Int.* **2015**, 960926 (2015).
17. L. Qiao, S. Hu, S. Liu, H. Zhang, H. Ma, K. Huang, Z. Li, T. Su, A. Vandergriff, J. Tang, T. Allen, P.-U. Dinh, J. Cores, Q. Yin, Y. Li, K. Cheng, MicroRNA-21-5p dysregulation in exosomes derived from heart failure patients impairs regenerative potential. *J. Clin. Invest.* **129**, 2237–2250 (2019).
18. Z. Li, S. Hu, K. Cheng, Chemical engineering of cell therapy for heart diseases. *Acc. Chem. Res.* **52**, 1687–1696 (2019).
19. Y. Chen, J. Huang, R. Chen, L. Yang, J. Wang, B. Liu, L. Du, Y. Yi, J. Jia, Y. Xu, Q. Chen, D. G. Ngondi, Y. Miao, Z. Hu, Sustained release of dermal papilla-derived extracellular vesicles from injectable microgel promotes hair growth. *Theranostics* **10**, 1454–1478 (2020).
20. H. Zhang, N.-X. Zhu, K. Huang, B.-Z. Cai, Y. Zeng, Y.-M. Xu, Y. Liu, Y.-P. Yuan, C.-M. Lin, iTRAQ-based quantitative proteomic comparison of early- and late-passage human dermal papilla cell secretome in relation to inducing hair follicle regeneration. *PLOS ONE* **11**, e0167474 (2016).
21. R. L. Rajendran, P. Gangadaran, S. S. Bak, J. M. Oh, S. Kalimuthu, H. W. Lee, S. H. Baek, L. Zhu, Y. K. Sung, S. Y. Jeong, S.-W. Lee, J. Lee, B.-C. Ahn, Extracellular vesicles derived from MSCs activates dermal papilla cell *in vitro* and promotes hair follicle conversion from telogen to anagen in mice. *Sci. Rep.* **7**, 15560 (2017).
22. Y. M. Choi, S. Y. Choi, H. Kim, J. Kim, M. S. Ki, I.-s. An, J. Jung, TGFβ family mimetic peptide promotes proliferation of human hair follicle dermal papilla cells and hair growth in C57BL/6 mice. *Biomed. Dermatol.* **2**, 23 (2018).
23. S. Hu, Z. Li, J. Cores, K. Huang, T. Su, P.-U. Dinh, K. Cheng, Needle-free injection of exosomes derived from human dermal fibroblast spheroids ameliorates skin photoaging. *ACS Nano* **13**, 11273–11282 (2019).
24. M. H. Kwack, C. H. Seo, P. Gangadaran, B.-C. Ahn, M. K. Kim, J. C. Kim, Y. K. Sung, Exosomes derived from human dermal papilla cells promote hair growth in cultured human hair follicles and augment the hair-inductive capacity of cultured dermal papilla spheres. *Exp. Dermatol.* **28**, 854–857 (2019).
25. B. H. Lee, J. S. Lee, Y. C. Kim, Hair growth-promoting effects of lavender oil in C57BL/6 mice. *Toxicol. Res.* **32**, 103–108 (2016).
26. S. Müller-Röver, B. Handjiski, C. van der Veen, S. Eichmüller, K. Foitzik, I. A. McKay, K. S. Stenn, R. Paus, A comprehensive guide for the accurate classification of murine hair follicles in distinct hair cycle stages. *J. Invest. Dermatol.* **117**, 3–15 (2001).
27. M. Ohyama, Y. Zheng, R. Paus, K. S. Stenn, The mesenchymal component of hair follicle neogenesis: Background, methods and molecular characterization. *Exp. Dermatol.* **19**, 89–99 (2010).
28. Y. Ito, T. S. Hamazaki, K. Ohnuma, K. Tamaki, M. Asashima, H. Okochi, Isolation of murine hair-inducing cells using the cell surface marker prominin-1/CD133. *J. Invest. Dermatol.* **127**, 1052–1060 (2007).
29. K. Cheng, W. S. Kisaalita, Exploring cellular adhesion and differentiation in a micro–/nano-hybrid polymer scaffold. *Biotechnol. Prog.* **26**, 838–846 (2010).
30. D. Shen, X. Wang, L. Zhang, X. Zhao, J. Li, K. Cheng, J. Zhang, The amelioration of cardiac dysfunction after myocardial infarction by the injection of keratin biomaterials derived from human hair. *Biomaterials* **32**, 9290–9299 (2011).
31. D. Shen, K. Cheng, E. Marbán, Dose-dependent functional benefit of human cardiosphere transplantation in mice with acute myocardial infarction. *J. Cell. Mol. Med.* **16**, 2112–2116 (2012).
32. Y. Lai, K. Cheng, W. Kisaalita, Three dimensional neuronal cell cultures more accurately model voltage gated calcium channel functionality in freshly dissected nerve tissue. *PLOS ONE* **7**, e45074 (2012).
33. N. Nagai, Y. Iwai, A. Sakamoto, H. Otake, Y. Oaku, A. Abe, T. Nagahama, Drug delivery system based on minoxidil nanoparticles promotes hair growth in C57BL/6 mice. *Int. J. Nanomedicine* **14**, 7921–7931 (2019).
34. M. P. Zimber, C. Ziering, F. Zeigler, M. Hubka, J. N. Mansbridge, M. Baumgartner, K. Hubka, R. Kellar, D. Perez-Meza, N. Sadick, G. K. Naughton, Hair regrowth following a Wnt- and follistatin containing treatment: Safety and efficacy in a first-in-man phase 1 clinical trial. *J. Drugs Dermatol.* **10**, 1308–1312 (2011).

35. L. Zhou, H. Wang, J. Jing, L. Yu, X. Wu, Z. Lu, Morroniside regulates hair growth and cycle transition via activation of the Wnt/β-catenin signaling pathway. *Sci. Rep.* **8**, 13785 (2018).
36. M. Bejaoui, M. O. Villareal, H. Isoda, β-catenin-mediated hair growth induction effect of 3,4,5-tri- *O*-caffeoylquinic acid. *Aging (Albany NY)* **11**, 4216–4237 (2019).
37. H. Yan, Y. Gao, Q. Ding, J. Liu, Y. Li, M. Jin, H. Q. Xu, S. Ma, X. Wang, W. Zeng, Y. Chen, Exosomal micro RNAs derived from dermal papilla cells mediate hair follicle stem cell proliferation and differentiation. *Int. J. Biol. Sci.* **15**, 1368–1382 (2019).
38. W.-h. Lin, L.-J. Xiang, H.-X. Shi, J. Zhang, L.-p. Jiang, P.-t. Cai, Z.-L. Lin, B.-B. Lin, Y. Huang, H.-L. Zhang, X.-B. Fu, D.-J. Guo, X.-K. Li, X.-J. Wang, J. Xiao, Fibroblast growth factors stimulate hair growth through β-catenin and shh expression in C57BL/6 mice. *Biomed. Res. Int.* **2015**, 730139 (2015).
39. P.-U. C. Dinh, D. Paudel, H. Brochu, J. Cores, K. Huang, M. T. Hensley, E. Harrell, A. C. Vandergriff, A. K. George, R. T. Barrio, S. Hu, T. A. Allen, K. Blackburn, T. G. Caranasos, X. Peng, L. V. Schnabel, K. B. Adler, L. J. Lobo, M. B. Goshe, K. Cheng, Inhalation of lung spheroid cell secretome and exosomes promotes lung repair in pulmonary fibrosis. *Nat. Commun.* **11**, 1064 (2020).
40. C. Hou, Y. Miao, J. Wang, X. Wang, C.-Y. Chen, Z.-Q. Hu, Collagenase IV plays an important role in regulating hair cycle by inducing VEGF, IGF-1, and TGF-β expression. *Drug Des. Devel. Ther.* **9**, 5373–5383 (2015).
41. H.-L. Xu, P.-P. Chen, L.-F. Wang, M.-Q. Tong, Z.-H. Ou, Y.-Z. Zhao, J. Xiao, T.-L. Fu, W. Xue, Skin-permeable liposome improved stability and permeability of bFGF against skin of mice with deep second degree scald to promote hair follicle neogenesis through inhibition of scar formation. *Colloids Surf. B Biointerfaces* **172**, 573–585 (2018).
42. Y. Qu, C. Cao, Q. Wu, A. Huang, Y. Song, H. Li, Y. Zuo, C. Chu, J. Li, Y. Man, The dual delivery of KGF and bFGF by collagen membrane to promote skin wound healing. *J. Tissue Eng. Regen. Med.* **12**, 1508–1518 (2018).
43. B. Zhao, Y. Chen, N. Yang, Q. Chen, Z. Bao, M. Liu, S. Hu, J. Li, X. Wu, miR-218-5p regulates skin and hair follicle development through Wnt/β-catenin signaling pathway by targeting SFRP2. *J. Cell. Physiol.* **234**, 20329–20341 (2019).
44. W. Chi, E. Wu, B. A. Morgan, Dermal papilla cell number specifies hair size, shape and cycling and its reduction causes follicular decline. *Development* **140**, 1676–1683 (2013).
45. T.-H. Young, H.-R. Tu, C.-C. Chan, Y.-C. Huang, M.-H. Yen, N.-C. Cheng, H.-C. Chiu, S.-J. Lin, The enhancement of dermal papilla cell aggregation by extracellular matrix proteins through effects on cell-substratum adhesivity and cell motility. *Biomaterials* **30**, 5031–5040 (2009).
46. C.-C. Yang, G. Cotsarelis, Review of hair follicle dermal cells. *J. Dermatol. Sci.* **57**, 2–11 (2010).
47. M. S. Orasan, I. I. Roman, A. Coneac, A. R. Muresan, R. I. Orasan, Hair loss and regeneration performed on animal models. *Clujul Med.* **89**, 327–334 (2016).
48. C. A. Jahoda, K. A. Horne, R. F. Oliver, Induction of hair growth by implantation of cultured dermal papilla cells. *Nature* **311**, 560–562 (1984).
49. C. A. Jahoda, R. F. Oliver, Vibrissa dermal papilla cell aggregative behaviour *in vivo* and *in vitro*. *J. Embryol. Exp. Morphol.* **79**, 211–224 (1984).
50. R. Schmidt-Ullrich, R. Paus, Molecular principles of hair follicle induction and morphogenesis. *Bioessays* **27**, 247–261 (2005).
51. C. A. Higgins, G. D. Richardson, D. Ferdinando, G. E. Westgate, C. A. B. Jahoda, Modelling the hair follicle dermal papilla using spheroid cell cultures. *Exp. Dermatol.* **19**, 546–548 (2010).
52. P. M. Plonka, D. Michalczyk, M. Popik, B. Handjiski, A. Slominski, R. Paus, Splenic eumelanin differs from hair eumelanin in C57BL/6 mice. *Acta Biochim. Pol.* **52**, 433–441 (2005).
53. Y. Zhang, Q. Liu, J. Yu, S. Yu, J. Wang, L. Qiang, Z. Gu, Locally induced adipose tissue browning by microneedle patch for obesity treatment. *ACS Nano* **11**, 9223–9230 (2017).
54. J. Zhu, X. Zhou, H.-J. Kim, M. Qu, X. Jiang, K. Lee, L. Ren, Q. Wu, C. Wang, X. Zhu, P. Tebon, S. Zhang, J. Lee, N. Ashammakhi, S. Ahadian, M. R. Dokmeci, Z. Gu, W. Sun, A. Khademhosseini, Gelatin methacryloyl microneedle patches for minimally invasive extraction of skin interstitial fluid. *Small* **16**, e1905910 (2020).
55. J. Yu, J. Wang, Y. Zhang, G. Chen, W. Mao, Y. Ye, A. R. Kahkoska, J. B. Buse, R. Langer, Z. Gu, Glucose-responsive insulin patch for the regulation of blood glucose in mice and minipigs. *Nat. Biomed. Eng.* **4**, 499–506 (2020).
56. J. Tang, A. Vandergriff, Z. Wang, M. T. Hensley, J. Cores, T. A. Allen, P.-U. Dinh, J. Zhang, T. G. Caranasos, K. Cheng, A regenerative cardiac patch formed by spray painting of biomaterials onto the heart. *Tissue Eng. Part C Methods* **23**, 146–155 (2017).
57. Q. Chen, C. Wang, X. Zhang, G. Chen, Q. Hu, H. Li, J. Wang, D. Wen, Y. Zhang, Y. Lu, G. Yang, G. C. Jiang, J. Wang, G. Dotti, Z. Gu, *In situ* sprayed bioresponsive immunotherapeutic gel for post-surgical cancer treatment. *Nat. Nanotechnol.* **14**, 89–97 (2019).

Acknowledgments: This work was performed, in part, at the Analytical Instrumentation Facility (AIF) at North Carolina State University, which is supported by the State of North Carolina and the NSF (award number ECCS-1542015). This work made use of instrumentation at AIF acquired with the support from the NSF (DMR-1726294). The AIF is a member of the North Carolina Research Triangle Nanotechnology Network (RTNN), a site within the National Nanotechnology Coordinated Infrastructure (NNCI). **Funding:** This work was financially supported by grants from the NIH (R01 HL123920, HL137093, HL144002, and HL146153 to K.C.) and the American Heart Association (18TPA34230092 and 19EIA34660286 to K.C.).
Author contributions: K.C. and S.H. designed the study. S.H. and Z.L. performed the experiments. S.H., H.L., K.H., T.S., J.C., and P.-U.C.D. analyzed the results and wrote the manuscript. J.C. finished grammatical edits. All the authors contributed to the overall scientific interpretation and edited the manuscript. **Competing interests:** The authors declare that they have no competing interests. **Data and materials availability:** All data needed to evaluate the conclusions in the paper are present in the paper and/or the Supplementary Materials. Additional data related to this paper may be requested from the authors.

Submitted 14 January 2020
Accepted 11 June 2020
Published 24 July 2020
10.1126/sciadv.aba1685

Citation: S. Hu, Z. Li, H. Lutz, K. Huang, T. Su, J. Cores, P.-U. C. Dinh, K. Cheng, Dermal exosomes containing miR-218-5p promote hair regeneration by regulating β-catenin signaling. *Sci. Adv.* **6**, eaba1685 (2020).